Fully Biodegradable and Biorenewable Ternary Blends from Polylactide, Poly(3-hydroxybutyrate-co-hydroxyvalerate) and Poly(butylene succinate) with Balanced Properties

Kunyu Zhang,[†] Amar K. Mohanty,[†,]* and Manju Misra*[,‡]

[†]Bioproducts Discovery and Development centre (BDDC), Department of Plant Agriculture, Crop Science Building, University of Guelph, Guelph N1G 2W1, Ontario, Canada

[‡]School of Engineering, Thornbrough Building, University of Guelph, Guelph N1G 2W1, Ontario, Canada

ABSTRACT: A ternary blend of entirely biodegradable polymers, namely polylactide (PLA), poly(3-hydroxybutyrate-co-hydroxyvalerate) (PHBV), and poly(butylene succinate) (PBS), was first melt-compounded in an effort to prepare novel fully biodegradable materials with an excellent balance of properties. The miscibility, morphology, thermal behavior, mechanical properties, and thermal resistance of the blends were investigated. DMA analysis revealed that PHBV and PLA showed some limited miscibility with each other, but PBS is immiscible with PLA or PHBV. Minor phase-separated structure was observed from SEM for all the blends composition except PHBV/PLA/PBS 60/30/10 blend, which formed a typical mixture of core–shell morphology. The morphologies were verified by analysis of the spreading coefficients. Excellent stiffness–toughness balance was achieved by ternary blends of PLA, PHBV, and PBS. Significant enhancement of the toughness and flexibility of PLA was achieved by the incorporation of PBS and PHBV without sacrificing the strength apparently. Both the stiffness and toughness were improved for PHBV in the ternary blends with PHBV as matrix. The crystallization of the PLA and PBS were enhanced by presence of PHBV in the blends, while the crystallization of PHBV was confined by PLA and PBS phases. Moreover, the thermal resistances and melt flow properties of the materials were also studied by analysis of the heat deflection temperature (HDT) and melt flow index (MFI) value in the work.

KEYWORDS: biodegradable polymer, ternary blends, Polylactide, Poly (3-hydroxybutyrate-co-hydroxyvalerate), Poly (butylene succinate)
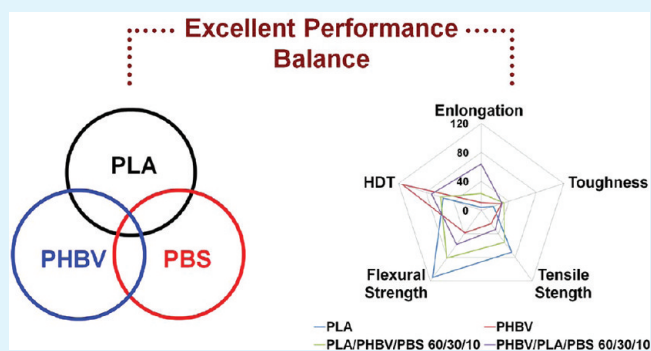
1. INTRODUCTION

Biodegradable polymers, especially biobased polymers derived from renewable resources, have attracted considerable attention in recent years because of the increasing concerns regarding environmental problems and shortages of our finite petroleum resources.[1−4] Among these polymers, biodegradable aliphatic polyesters such as polylactide (PLA), polyhydroxyalkanoates (PHAs), and poly(butylene succinate) (PBS) have been intensively studied due to their biodegradability, biocompatibility and commercial availability in market. More appealingly, these new polymers have the inherent advantage of being produced from renewable resources such as cellulose and starch, and if their end-of-life scenario is properly designed by using recycling or composting, their environmental footprint can be reduced.[5] With the innovative technology development and the decreasing costs, these eco-friendly polymers will successfully compete as sustainable replacements to traditional petroleum-based products.

PLA is one kind of thermoplastic aliphatic polyester derived from nonfossil renewable natural resources such as starch.[6] As the most popular biodegradable polymer, PLA has been widely used in biomedical applications because of its biodegradability and biocompatibility. Recently, the inexpensive price of industrial grade PLA along with its high mechanical strength and good processability enables it to be used as a sustainable alternative to petrochemical-derived products in commodity applications.[7−9] However, neat PLA exhibits brittleness and its fracture strain is only about 5% in the tensile test, which results in poor impact and tear resistance.[8−13] In addition, it also shows poor heat stability with low levels of heat deflection temperature (HDT). These inherent deficiencies of PLA have significantly hindered its large-scale applications in both commodity and biomedical areas.

Another widely studied bioresourced family of polymer is bacterial polyhydroxyalkanoates. PHAs are natural biodegradable thermoplastics produced as intracellular energy and carbon

storage materials by various microorganisms.[14,15] To date, only a few PHAs, mainly polyhydroxybutyrate (PHB) and poly(3-hydroxybutyrate-co-hydroxyvalerate) (PHBV), are commercially available and produced on an industrial scale. In the family of PHAs, PHBV has gained a lot of attentions because of its remarkable features including its excellent biodegradability, biocompatibility, and some properties similar to those of polypropylene.[16] Moreover, compared to other biodegradable polyesters, PHBV shows excellent thermal resistance ability due to its high crystallinity. These fascinating properties make PHBV a potential substitute for petroleum-based polyolefins in many areas.[17] Nevertheless, widespread application of PHBV is also limited because of its brittleness, low impact resistance, and high production cost.[18]

Being different from PLA and PHBV, poly(butylene succinate), a commercially available aliphatic polyester synthesized via chemosynthetic way, exhibits excellent flexibility and toughness.[19,20] PBS is usually synthesized via polycondensation of 1, 4-butanediol with succinic acid, which can be derived from fossil-based or renewable resources.[19] Especially in recent years, renewable-based PBS has made tremendous progress with breakthrough biotechnology in commercial production of its important feedstock, succinic acid from renewable resources.[21] PBS possesses many interesting properties, including biodegradability, melt processability, and thermal and chemical resistance.[20] PBS is thus attracting attention as a promising eco-friendly alternative to common plastics. However, other properties of PBS, such as stiffness, gas barrier properties, and melt viscosity for further processing, are often not sufficient for various end-use applications.

As noted above, PLA, PHBV and PBS represent the most promising candidates for future developments and play key roles in the marketing of biodegradable polymers designed for various potential applications. Nevertheless, none of these three polymers can fulfill the requirement for almost all structural materials in commercial application when used alone. However, it is notable that PLA, PHBV and PBS show very interesting complementary properties. These complementary properties among PLA, PHBV, and PBS blend components are very important and interesting that one can tailor the mechanical properties, processing properties and thermal performance by a simple melt blending method. Polymer blends have been widely used in the industry because of their ability to combine in a unique material the properties of their components, at a relatively low cost when compared to the development of a new polymer. Many studies have been done to improve the physical properties of the neat polymers by binary blends between PLA, PHBV or PBS.[22−31] Some interesting and noteworthy results have been introduced in recent reports. However, the major drawbacks of binary blends are the substantial decreases in one property when improving the other properties such as the strength and modulus of the toughened materials. The development of biopolymer blends with appropriate melt strength, stiffness-toughness balance, and requisite thermal performance is still elusive. Compared to binary blends, multicomponent polymer materials usually exhibit more excellent balance performance. Recently, the study and development of multicomponent polymer blends formed by three or more components has gained the attention of both the industrial and the academic world.[32−42] Novel high-performance materials arising from synergistic interactions can be achieved by combining different plastics with complementary properties.[32,39,42,43] However, very little attention has been paid

to ternary or multicomponent polymer blends from biopolymers.[42] To the best of our knowledge, no research about the ternary blends of PLA, PHBV, and PBS has been reported so far. Considering the promising complementary properties among PLA, PHBV and PBS blend components, in the present work, we focus on ternary blends of PLA/PHBV/PBS by simple melt blending method to obtain Bioplastic blends with good balance performance. To gain biopolymer blends with the appropriate melt strength, stiffness−toughness balance along with requisite thermal performance, the PLA or PHBV was used as matrix, respectively, whereas PBS was used as minor phase in the blends to improve the toughness. The miscibility, crystallization behavior, phase morphology, mechanical properties, and thermal resistance of the multicomponent system were investigated.

2. EXPERIMENTAL SECTION

2.1. Materials. The PLA (Natureworks PLA 3251D) used in this study was purchased from Nature Works LLC, USA. It exhibits a weight-average molecular weight ($\bar{M}_w$) of 5.5×10^4 g/mol and polydispersity index (PI) of 1.62 (GPC analysis). The PHBV ($\bar{M}_w$ = 2.9×10^5 g/mol and PI = 1.62) used in this work is a product from Telles Inc. with the trade name of Mirel P1004 donated to us by Competitive Green Technologies, ON, Canada. The Mirel P1004 grade consists of additives, and mineral fillers. PBS ($\bar{M}_w = 1.4 \times 10^5$ g/mol and PI = 1.82), commercially named Bionolle 1020, was supplied from Toyo Plastics Co., Ltd., Japan, manufactured by Showa Highpolymer Co. Ltd., Japan. The chemical structures of the three polymers used for the blends are illustrated in Scheme 1.

Scheme 1. Illustration of the Chemical Structure of the Three Polymers
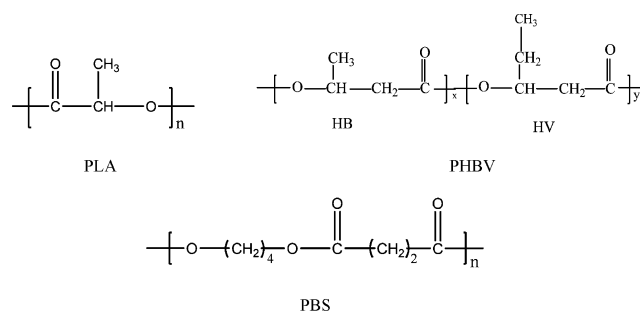
2.2. Preparation of the Blends. Prior to blending, all the materials were dried at 80 °C in the oven for at least 4 h. Blends of PLA/PHBV/PBS of varying compositions were compounded in a corotating twin screw microcompounder from DSM-Xplore (DSM, Netherlands). The miro-extruder used in this work has a screw length of 150 mm, an L/D of 18, and a barrel volume of 15 cm³. The extrusion parameters were barrel temperature = 180 °C, screw speed = 100 rpm, residence time = 2.5 min, until the viscosity had reached a nearly constant value. The molten blend material was transferred from a mini-extruder to a preheated small injection molder for fabrication of various test specimens. Also the neat PLA and PHBV were subjected to the mixing treatment so as to have the same thermal history as the blends.

2.3. Dynamic Mechanical Analysis (DMA). DMA was carried out with a DMA Q800 from TA Instruments. A dual cantilever clamp was used at the frequency of 1 Hz and oscillating amplitude of 15 mm. The samples were heated from −50 to 120 °C at a heating rate of 3 °C/min.

2.4. Scanning Electron Microscope (SEM) and Transmission Electron Microscopy (TEM). The morphology of the blends was observed by a Hitachi S-570 SEM with an accelerating voltage of 15 KV. The samples were cooled in liquid nitrogen, and then broken.

Then the specimen was mounted on an aluminum stub using a conductive paint and finally sputtered with gold prior to fractographic examination. The fracture surfaces obtained from the notched Izod impact test were also characterized by SEM.

Transmission electron microscopy (TEM) was also used to observe the phase morphology of the blends. TEM was performed using a JEOL-2010F transmission electron microscope (TEM, JEOL, Tokyo, Japan) with 200 kV accelerating voltage. Ultrathin sections (70−90 nm) for TEM studies were obtained using an ultramicrotome with a diamond knife at −40 °C.

2.5. Differential Scanning Calorimetry (DSC). DSC measurements were performed on a TA Q200 DSC instrument under N_2 atmosphere. First, the samples were heated to 190 °C with a heating rate of 10 °C/min, and maintained at that temperature for 3 min before cooling to −50 °C at a rate of 20 °C/min and 2 °C/min. After that, the second heating scans were monitored between −50 to 190 °C at a heating rate of 10 °C/min for determining glass transition temperature (T_g), cold crystallization temperature (T'_m) and melting temperature (T_m).

2.6. Mechanical and Impact Analysis. Tensile and flexural tests were performed at room temperature using an Instron universal testing machine, model 3382 according to ASTM standards D638 and D790, respectively. Also, Izod impact testing of notched samples was carried out as per ASTM D256 by a Testing Machine Inc. (TMI) instrument. In all mechanical tests, the reported data are the mean and standard deviation from at least 5 measurements. All samples were conditioned for 72 h at 23 °C and a relative humidity of 50%.

2.7. Wide-Angle X-ray Diffraction (WAXD). Wide angle X-ray diffraction analysis (WAXD) experiments were performed on Rigaku X-ray diffractometer. The measurements were operated at 40 kV and 20 mA from 2°-40° at a 2θ scan rate of 2°/min. Here the samples for WAXD were subjected to the same thermal history as the DSC measurement with cooling rate at 20 °C/min.

2.8. Heat Deflection Temperature (HDT). The same instrument and samples as for DMA were applied for HDT measurements in three-point bending mode at a constant applied load of 0.455 MPa. The samples were heated from room temperature to the desired temperature with a ramp rate of 2 °C/min. The HDT was reported as the temperature at which a deflection of 0.25 mm occurred.

2.9. Melt Flow Index (MFI). Melt flow index (MFI) of the polymer and the blends was determined according to ASTM D1238 at 190 °C with a load of 2.16 kg by using a Melt Flow Indexer (Qualitest model 2000A).

3. RESULTS AND DISCUSSION

3.1. Tensile and Flexural Properties of PLA/PHBV/PBS Blends. Figure 1 shows the representative strain−stress curves of neat PLA, PHBV and the ternary blends. Neat PLA is a very rigid polymer and deforms in brittle fashion. No obvious yield
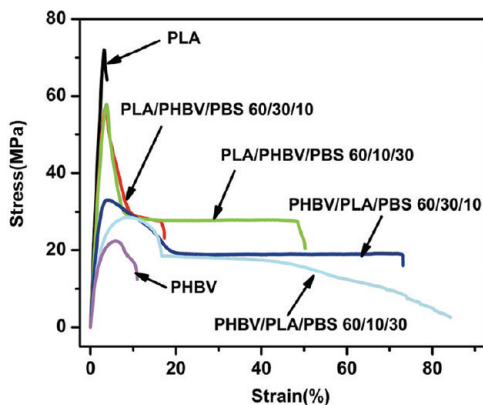

Figure 1. Tensile stress−strain curves of neat PLA, PHBV, and PLA/PHBV/PBS ternary blends.

was observed from the strain−stress curves, and the elongation at break was only about 4%. Compared to PLA, pure PHBV showed a slightly better flexibility with elongation above 10%. However, the strength of PHBV was poor and only at 22.2 MPa. The ternary blends showed an excellent balance in tensile properties in comparison to the neat polymer. It is notable that all the ternary blends underwent distinct yielding and considerable cold drawing after the yielding. This result indicates that the fracture behavior of the ternary blends specimen displayed a transition from brittle fracture to ductile fracture.

The comparative tensile strength and modulus of PHBV, PLA, and the ternary blends are shown in Figure 2, while the
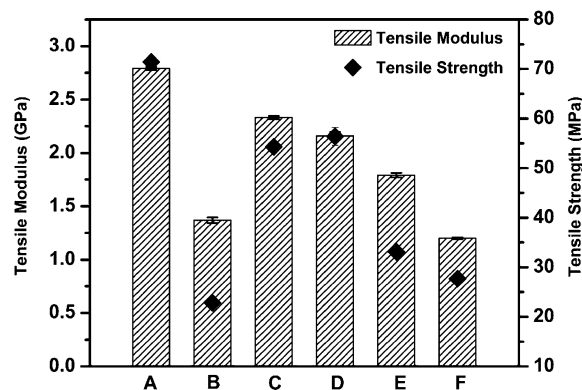

Figure 2. Tensile modulus and strength of PLA/PHBV/PBS ternary blends as function of the weight fraction: (A) neat PLA; (B) neat PHBV; (C) PLA/PHBV/PBS 60/30/10; (D) PLA/PHBV/PBS 60/10/30; (E) PHBV/PLA/PBS 60/30/10; (F) PHBV/PLA/PBS 60/10/30.

evolution of the elongation at break and impact strength with composition are reported in Figure 3. As presented here, for the
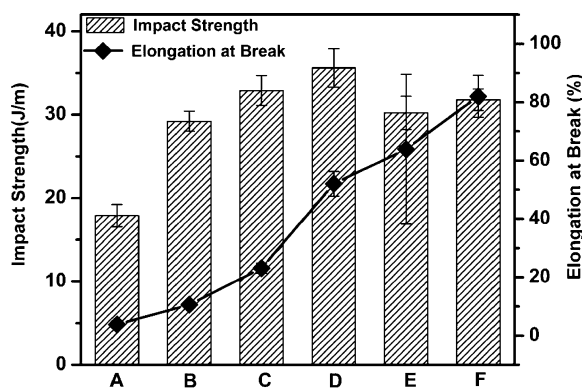

Figure 3. Notched Izod impact strength and percent elongation at break of PLA/PHBV/PBS ternary blends as function of the weight fraction: (A) neat PLA; (B) neat PHBV; (C) PLA/PHBV/PBS 60/30/10; (D) PLA/PHBV/PBS 60/10/30; (E) PHBV/PLA/PBS 60/30/10; (F) PHBV/PLA/PBS 60/10/30.

blends with PLA as matrix, blending a small amount of PHBV and PBS was able to considerably improve the flexibility of PLA with moderate reducing its tensile strength. The elongation of the PLA/PHBV/PBS 60/30/10 blend reached 23%, increasing by above 5 times over that of neat PLA, while the yielding stress remained 54.3 MPa, slightly lower than that of neat PLA. When 10 wt % PHBV and 30 wt % PBS were added, the elongation at

3093

dx.doi.org/10.1021/am3004522 | *ACS Appl. Mater. Interfaces* 2012, 4, 3091−3101

break of the blend further increased and reached above 50%, increasing by more than 10 times over that of neat PLA with almost no change in the strength and modulus. The tensile strength and modulus of the PLA/PHBV/PBS blends decreased by increasing PHBV and PBS content as expected due to the incorporation of a soft phase to the PLA matrix. This trend was also observed in flexural properties of the blends, which are shown in Figure 4. The flexural data obtained is
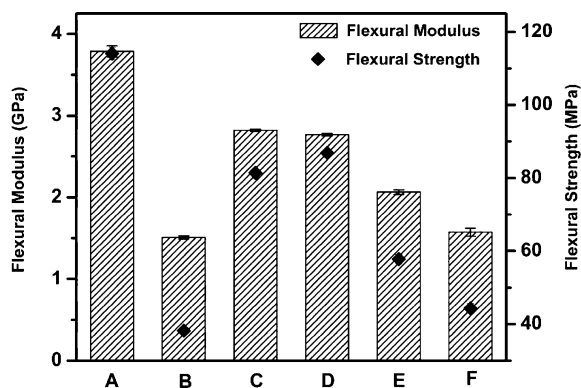

Figure 4. Flexural modulus and strength of PLA/PHBV/PBS ternary blends as function of the weight fraction: (A) neat PLA; (B) neat PHBV; (C) PLA/PHBV/PBS 60/30/10; (D) PLA/PHBV/PBS 60/10/30; (E) PHBV/PLA/PBS 60/30/10; (F) PHBV/PLA/PBS 60/10/30.

consistent with the tensile data, showing a slightly decrease in flexural strength and flexural modulus. For blends, the nature and extent of bonding between the various phases critically

determines the mechanical strength and other properties of the materials.[11,12] When the sample is subjected to the tensile stress during the tensile test, the domains of soft PBS and PHBV might act as stress concentrators because of the different elastic property of PBS or PHBV from that of PLA. The stress concentration resulted in high triaxial stress in the domains, especially in PBS domains, and the debonding occurred at the particle−matrix interface due to insufficient interfacial adhesion.[13] The interfacial cavitations led to a relief of the triaxial stress state of the matrix around the voids, thus creating a stress state beneficial for the initiation of multiple matrix shear yielding.[11,44] As the yielding of the matrix occurred, the stress was then applied to the PBS domains. Then, as the debonding progressed, the orientation of both the matrix and the dispersed domains occurred.

The attainment of both strength and toughness is a vital requirement for most structural materials, unfortunately, these properties are generally mutually exclusive. Usually, toughening of a polymer matrix material is accompanied by a drastic reduction in strength for binary blends. This trend is also true for the binary blends of PLA, PHBV and PBS.[22−31] However, this unique phenomenon of increased toughness with improved strength was achieved for ternary PHBV/PLA/PBS blends with PHBV as the matrix, whereas PLA and PBS as the minor phases in this work. Interestingly, both the stiffness and flexibility were significantly improved compared to neat PHBV by the introduction of the PLA and PBS as minor phases. In the blends PHBV/PLA/PBS 60/30/10, the presence of PLA and PBS minor phases enhanced the strength of PHBV from 22.2 to 33 MPa, and elongation at break was increased from 10 to 64%. Better flexibility was achieved for the PHBV/PLA/PBS
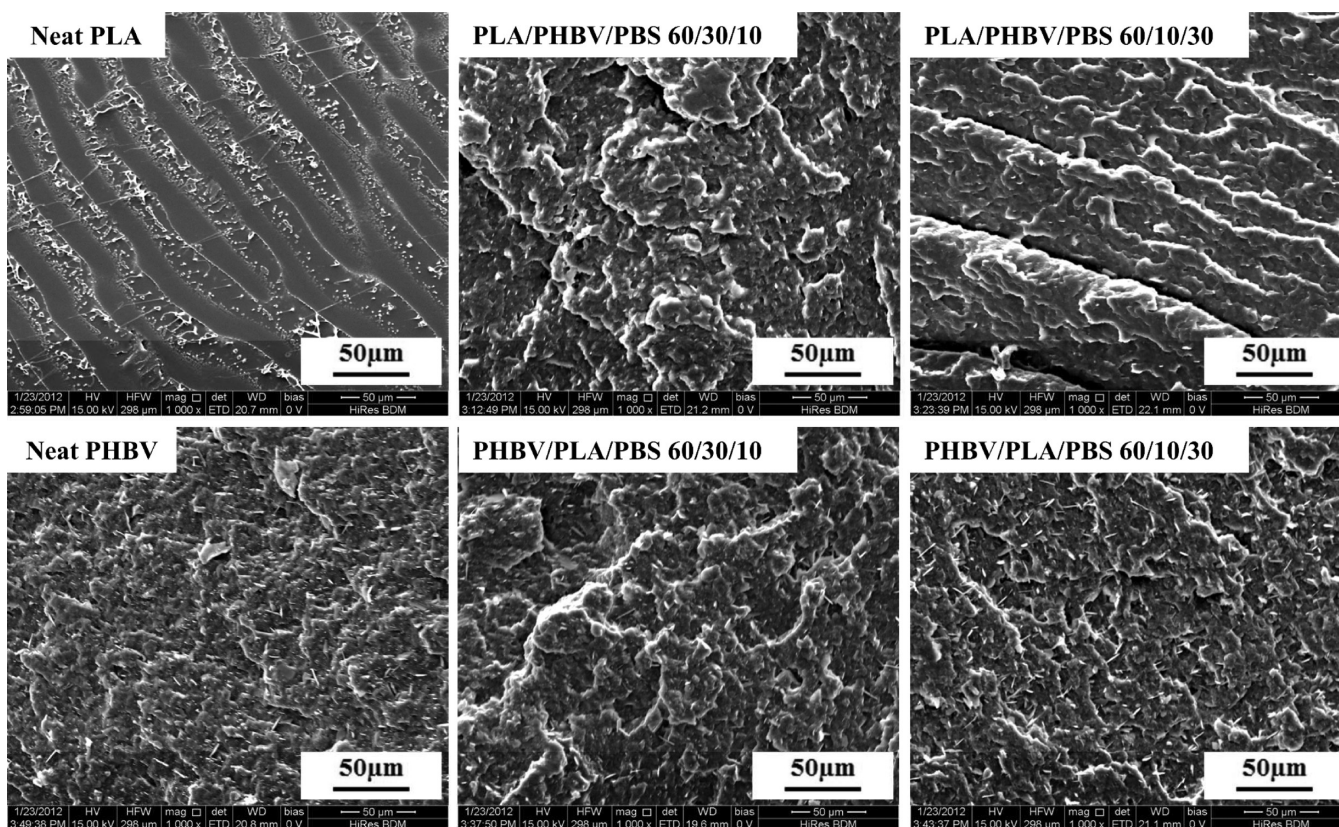

Figure 5. SEM images of impact-fracture surface of PLA/PHBV/PBS ternary blend with various weight compositions.

60/10/30 with elongation at break at 82% and strength at 28 MPa. Flexural strength and modulus are important indicators for the stiffness of polymers. In consistent with the tensile strength and modulus, a considerable improvement in flexural properties is also observed for the ternary blends compared with PHBV alone. As shown in Figure 4, neat PHBV exhibits low flexural strength value (38 MPa) and modulus (1509 MPa). With the addition of 10% PLA in PHBV/PLA/PBS 60/10/30 blend, the flexural strength and modulus increased to 44 and 1543 MPa, respectively. More significant increase in the flexural strength and modulus is observed for the PHBV/PLA/PBS 60/30/10 blend with fraction of 30% PLA: the flexural strength and modulus ramps up to 58 and 2064 MPa, respectively. The striking mechanical performance could be attributed to the synergistic effect played by PLA and PBS phases. In the ternary blends with PHBV as matrix, high stiff PLA minor phases play a role as a strengthen agent for PHBV,[29] whereas the flexible PBS perform as a toughening agent. The interplay of these two phases with PHBV matrix leads to a good balance of mechanical properties for PHBV/PLA/PBS ternary blends. Such a combination of properties, good flexibility, and high stiffness, is impossible to be attained by classical binary blends. These results are very significant in obtaining a biobased material having a remarkable stiffness-toughness balance. On the basis of the above-described mechanical results, it is found that the PLA/PHBV/PBS 60/10/30 and PHBV/PLA/PBS 60/30/10 show optimum balance of mechanical performance. This unique combination of properties should open applications hitherto inaccessible to neat PHBV, PLA, and PBS alone.

3.2. Impact Strength. The impact strength evaluation is an important tool to study the fracture toughness of polymer blends. Figure 3 also compares the impact strength of neat polymer with that of the blends at room temperature. All the blends clearly showed higher impact strength than that of neat polymer, especially for the blends with PLA as matrix. The impact strength of neat PLA was only about 17 J/m, and the samples clearly fractured in a brittle manner. In the case of ternary blends with PLA as matrix, the introduction of PHBV and PBS increase the impact strength of PLA. It seems that PBS is more effective than PHBV when used as an impact modifier for PLA in the blends. An increase in the concentration of PBS in the blends resulted in a gradual increase in toughness in the blends. Significant improvement can be observed for blends PLA/PHBV/PBS 60/10/30 with 30 wt % PBS, which was approximately 2 times higher than that of neat PLA. It is well-known that toughness implies energy absorption and can be achieved through addition of a second flexible phase in the form of particles. The phase-separated particles, especially after the cavitation process, induce large stress concentrations which lead to extensive shear deformation, a high-energy-absorbing mechanism.[11,12] To further study the toughening effect of PLA/PHBV/PBS ternary blends, the fracture surface of the impact specimen was investigated by SEM, and the results are shown in Figure 5.

The structure of the fracture surface and the stress whitened zone provides direct information about the occurring deformation mechanism and the stability of the propagating crack on loading. Pure PLA showed a smooth and featureless fracture surface without much deformation, indicating a typical brittle fracture behavior. The fracture surfaces of the blends became increasingly rough with an increasing concentration of PBS. Many irregularities can be observed for the blend with

10% PBS. When PBS content was up to 30 wt %, the structure of the fracture surface became more rugged and consisted of more strongly deformed, fibrillated material. These results indicated that the matrix shear yielding had clearly occurred and deformed the PBS particles. The corresponding amount of plastic deformation is high and effectively dissipates the fracture energy, which results in highly improved impact strengths at room temperature. Similar results were also found for the ternary blend with PHBV as matrix; the impact strength was increased by introduction of PBS phases. However, the improvement of impact strength is not as significant for the blends compared to that for PHBV, which may be due to the poor interfacial adhesion between the PHBV and PBS.

3.3. Dynamic Mechanical Properties. Figure 6A shows the storage modulus curves of neat PLA, PHBV, and the
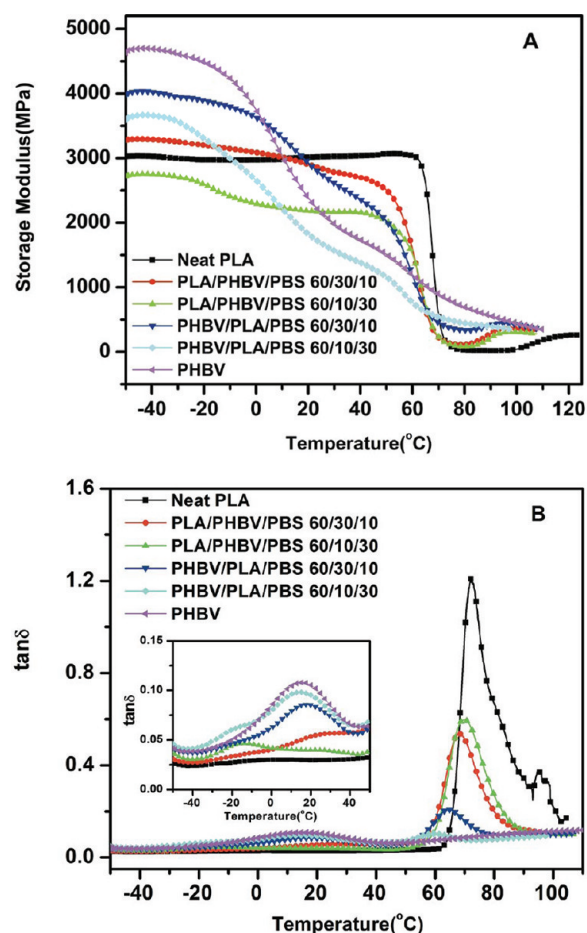

Figure 6. DMA traces of PLA/PHBV/PBS ternary blends at various concentrations: (A) storage modulus versus temperature; (B) tan δ versus temperature versus.

ternary blends. The storage modulus (E') of PLA at room temperature was about 3 GPa, in agreement with the value for a glassy polymer. The glass transition of PLA started at about 68 °C, and the storage modulus accordingly decreased sharply. At the glass transition temperature (T_g), the storage modulus E' of PLA decreased more than 1 order of magnitude, reaching a value below 300 MPa. Then, the cold crystallization happened at around 120 °C, and as the result of crystallization, the storage modulus increased. Neat PHBV showed highest storage modulus at the temperature range below its T_g. When the temperature increased above its T_g, the storage modulus (E') of

PHBV decreased sharply due to the occurrence of glass transition. It was found that the E' of PHBV showed a lower value than that of PLA at room temperature. In the case of the ternary blends, the blends with high content of PLA showed a higher storage modulus above room temperature and increased with increasing content of PLA. However, below the T_g of PHBV, the blends with higher concentration of PHBV exhibited higher modulus. Moreover, it was interestingly found that the temperature at which E' started to increase, due to the cold-crystallization of PLA component, shifted to a lower temperature with the addition of PHBV and PBS. This result suggests that the incorporation of PHBV and PBS enhances the cold-crystallization ability of PLA, which is consistent with the following results of the DSC.

Tan delta (tan δ) is the ratio between the loss modulus (E'') and the storage modulus (E'). In tan δ, a peak is observed at a region where the rate of decrease in storage modulus is higher than that of loss modulus with increase in temperature. This peak is the transition in molecular mobility representing the T_g of the substance. The glass transition temperature of a polymer blend is one of the most important criteria for the miscibility of components. Consequently, DMA was employed to assess the miscibility of the polymer blends, and the data for tanδ of the blends are shown in Figure 6B. As shown in Figure 6B, a sharp tan δ peak was observed around 68 °C for neat PLA, corresponding to its glass transition. A clear shift in the tanδ peak toward the lower end of temperature range can be observed for the blends with the increased concentration of PHBV and PBS. These results suggest that PLA shows limited miscibility with PHBV and PBS minor phases. By careful analysis of these results, it was found that the T_g of PLA and PHBV shifted to each other remarkably when the concentration varied. However, for the T_g of PBS, no big change is seen with the concentration varied. This result demonstrates that compared to PBS, PLA showed better miscibility with PHBV, implying that there is better interfacial interaction between PLA and PHBV.

3.4. Phase Morphology of the Ternary Blends.
As is well-known, phase behavior plays a vital role in mechanical behavior of polymer blends. The types of morphology and the size of dispersed phases in the polymer blends are important factors that determine physical properties and rheological behavior. Furthermore, phase morphology can provide the relationship between microstructure and the mechanical properties. Scanning electron microscope (SEM) and transmission electron microscopy (TEM) are mostly important method to characterize the morphology of multiphases blends. Therefore, the detailed phase morphology of the blends was studied by SEM and TEM method. Figure 7 presents the SEM micrographs of cryo-fractured surfaces of PLA/PHBV/PBS ternary blends. As shown in the graphs, PHBV and PBS particles and dark holes left by them during fracture were observed on the surface of the PLA/PHBV/PBS blends with PLA as matrix. PHBV and PBS phase domains preferentially separately dispersed as spheres in the continuous PLA matrix with somewhat indistinct surface. The approximate diameters of the dispersed minor phases were in the order of submicrometer in the blends. The surface of these particles is smooth with clear borders, suggesting poor compatibility and weak interfacial adhesion between the phases. However, the phase behavior of PHBV/PLA/PBS blends with PHBV as matrix contrast strongly with that of PLA/PHBV/PBS blends. A typical core−shell morphology with PLA as shell and PBS as
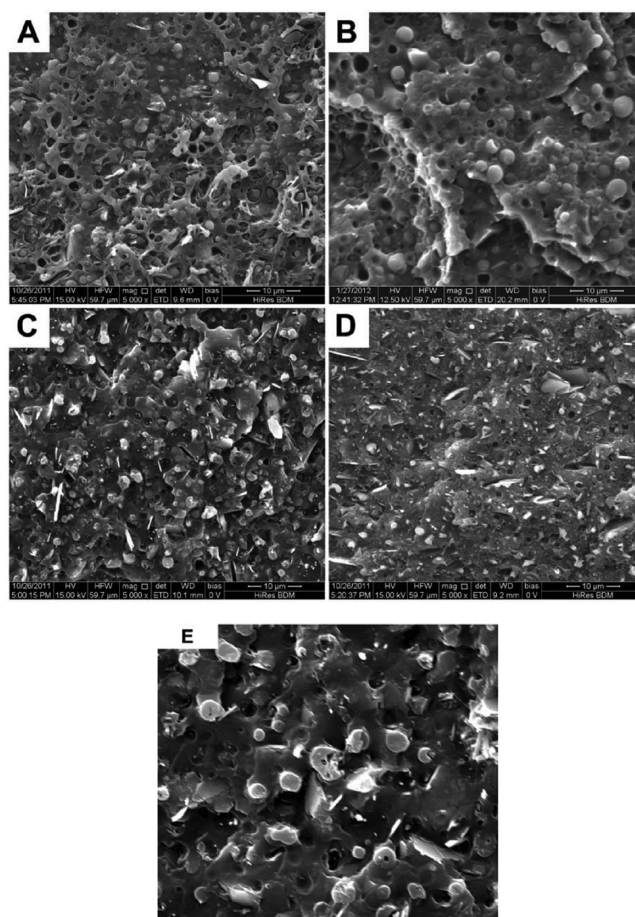

Figure 7. SEM images of cryofractured surface of PLA/PHBV/PBS blend with various weight compositions: (A) PLA/PHBV/PBS 60/30/10; (B) PLA/PHBV/PBS 60/10/30; (C) PHBV/PLA/PBS 60/30/10; (D) PHBV/PLA/PBS 60/10/30 (E) PHBV/PLA/PBS 60/30/10 with high magnification of 10 000.

core was observed for blends PHBV/PLA/PBS 60/30/10. When the content of PLA and PBS changed, different morphology with separated-phases structure was observed again.

Figure 8 shows the TEM micrographs of the ternary blend. It should be noted that PLA, PHBV, and PBS belong to the same family of aliphatic polyester with similar chemical and physical properties. The PLA, PHBV, and PBS show only slight difference in the density, which result in small elastic electron scattering discrepancy during the TEM experiments. The very small elastic electron scattering discrepancy among these three components make it be difficult to distinguish each other by TEM image, especially for the two minor phases in the ternary blends. As shown in Figure 8, phase-separated minor phase morphology was observed for the blends with PLA as the matrix and the blend PHBV/PLA/PBS 60/10/30, which is in consistent with the SEM results. The diameters of the different dispersed minor phases were in the order of submicrometer in the blends and varied with the concentration of the minor phases changed. Based on the diameter and the composition, it can roughly distinguish the minor phases. For example, in the PLA/PHBV/PBS 60/30/10, the larger granule shown in the picture may be attributed to PHBV phase considering its higher concentration. The larger and more irregular morphology in the PLA/PHBV/PBS 60/10/30 may be due to the deformation
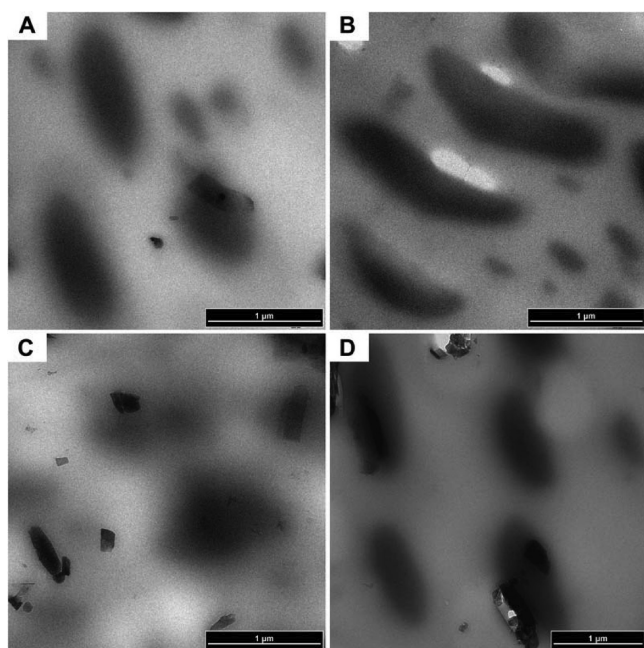
3096

dx.doi.org/10.1021/am3004522 | ACS Appl. Mater. Interfaces 2012, 4, 3091−3101

Figure 8. TEM images of PLA/PHBV/PBS blends with various weight compositions: (A) PLA/PHBV/PBS 60/30/10; (B) PLA/PHBV/PBS 60/10/30; (C) PHBV/PLA/PBS 60/30/10; (D) PHBV/PLA/PBS 60/10/30.

of the soft PBS during the cutting. Consistent with SEM results, a relative uniform dispersion can be observed for the PHBV/PLA/PBS 60/10/30 blend. However, for the blend PHBV/PLA/PBS 60/30/10 with core−shell morphology, it is difficult to distinguish the morphology of minor phases because of the small density discrepancy among the three components. Without the suitable staining method, the poor contrast of the minor phase makes it a great challenge to characterize the morphology of the ternary blends.

Most of the researches on the subject of multiphase blends show that the morphology of ternary blends can be predicted through the knowledge of interfacial tension between the components of the blends.[34−41] In particular, Hobbs et al.[37] used the concept of the spreading coefficient and rewrote Harkin's equation, in which two distinct phases are dispersed in a matrix phase, to predict the morphology of ternary blends. In a ternary blend of three polymers 1, 2, and 3 (supposing 2 is the matrix), the spreading coefficient, λ_{31} can be defined as

$$\lambda_{31} = \gamma_{12} - \gamma_{32} - \gamma_{13} \qquad (1)$$

Where λ_{31}, is the spreading coefficient of 1 over 3 and Y_{ij} is the interfacial tension between r and j. For 1 to be encapsulated by 3, λ_{31} must be positive. In the case when both λ_{31} and λ_{13} are negative, 1 and 3 will tend to form separated phases. To correlate the phase morphology and the interfacial tension between the constitutive components, the values of γ_{12}, γ_{32}, γ_{13} have been estimated by using the harmonic mean equation[40] at the mixing temperature (180 °C)

$$\gamma_{12} = \gamma_1 + \gamma_2 - 4\left[\frac{\gamma_1^d \gamma_2^d}{\gamma_1^d + \gamma_2^d} + \frac{\gamma_1^P \gamma_2^P}{\gamma_1^P + \gamma_2^P}\right] \qquad (2)$$

The surface parameter values of PLA, PHBV, and PBS at 180 °C were extrapolated from the experimental values, 25 °C, by using the common temperature coefficient of −0.06 mJ m^{-2}

K^{-1}.[32,40] Surface tension data of polymers at the mixing temperature are listed in Table 1. All these data are available in

Table 1. Estimated surface tension of polymers at the mixing temperature (180 °C)

polymer	γ_s (mN/m)	γ_d (mN/m)	γ_p (mN/m)
PHBV	32.6	31.7	0.9
PLA	34	30	4
4PBS	46.4	32.4	14

the scientific literature for PHBV, PLA, and PBS.[45,46] The spreading coefficients were calculated from the surface tension data at 180 °C based on the eq 1 and the results are shown in Table 2. Taking the PHBV/PLA/PBS 60/30/10 blends as an

Table 2. Estimated Spreading Coefficients at 180 °C from the Interfacial Tensions

sample (wt/wt/wt)	λ_{31} (mN/m)
PLA/PHBV/PBS(60/30/10)	−8.0
PLA/PHBV/PBS (60/10/30)	−13.1
PHBV/PLA/PBS (60/30/10)	3.83
PHBV/PLA/PBS(60/10/30)	−15.2

example with PHBV as matrix 2, PLA as shell 3, and PBS as core 1, it can be calculated that the λ_{31} is 3.83 mN/m, indicating that the PBS is encapsulated by PLA. As shown in Figure 7C, E, in agreement with the calculation, a core−shell structure has been clearly observed for the blend PHBV/PLA/PBS 60/30/10. An excellent stress transfer among the three phases may occur because of the favorable interfacial adhesion of PLA with matrix PHBV, which may result in the good mechanical properties of the blend PHBV/PLA/PBS 60/30/10.[39,42,43] For the other blend compositions, it was found that all the spreading coefficient values were negative, indicating that the minor phases tend to form separated phase morphology.

3.5. Thermal and Crystallization Behaviors of PLA/PHBV/PBS Ternary Blends. PLA, PHBV, and PBS are typical semicrystalline polymers. The physical, mechanical, and thermal resistance properties of these polymers are greatly dependent on the solid-state morphology and its crystallinity. Accordingly, it is very important to study the influence of the existence of the other minor components on the crystallization of matrix polymers in the blend. Figure 9 shows the DSC cooling thermograms at a cooling rate of 20 °C/min for neat polymers and the blends after being melted at 190 °C for 3 min. Neat PLA showed no exothermic peak corresponding to the crystallization of the PLA component at this cooling rate, indicating that the PLA was primarily amorphous when cooling down from melt at the cooling rate of 20 °C/min. However, obvious exothermic peaks can be observed for neat PHBV and PBS from the thermograms. The crystallization peak temperature (T_c) of neat PHBV is around 105 °C, whereas T_c of neat PBS is around 72.3 °C at a cooling rate of 20 °C/min. Comparing the curves of the blend with neat polymers, it could be observed that crystallization temperature of PHBV (T_c) shifted to low temperature, indicating that the crystallization of PHBV was restricted by the presence of PLA and PBS phases. Such results can be explained by the reason that the presence of PLA and PBS suppressed the nucleation of PHBV in the blends. The number of heterogeneous primary nuclei of PHBV may decrease because of the migration of heterogeneity from
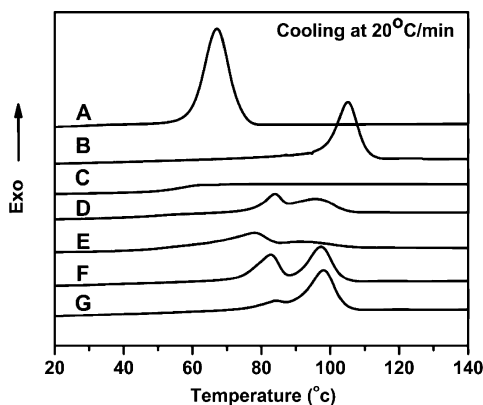
Figure 9. Cooling DSC thermograms at cooling rate 20 °C/min for neat polymer and the blends after melted at 190 °C for 3 min: (A) PBS; (B) PHBV; (C) PLA; (D) PLA/PHBV/PBS (60/30/10); (E) PLA/PHBV/PBS (60/10/30); (F) PHBV/PLA/PBS (60/30/10); (G) PHBV/PLA/PBS (60/10/30).

PHBV to PLA and PBS. Similar results were also reported recently on the crystallization behavior of other PHBV-based blends, such as PHBV/PCL, PHBV/PBS, or PES, etc.[47−50] Another possible reason, especially in the case of blends with PLA as matrix, for the decrease of the crystallization growth rate of PHBV here is that it could be caused by the dilution effect of PLA and PBS melt, which reduces the amount of PHBV chain segments toward the growing crystals.[50] Contrary to crystallization behavior of PHBV in the blends, the T_c of PBS in the blends shifted to a high temperature, indicating that the crystallization of PBS was promoted in the blends. It can be found that the crystallization of PHBV takes place prior to that of PBS. PBS crystallized in a phase-separated system, where PHBV existed as a solid crystallization phase. It is reasonable to speculate that PHBV forms small-dispersed crystals during the cooling process, which may act as nucleation sites of PBS. Consequently, the improvement in crystallization of PBS may be attributed to the positive effect played by PHBV crystals on the nucleation of PBS.

Figure 10 presents the second heating thermograms of neat polymer and the ternary blends after cooling at 20 °C/min. As shown in Figure 10, neat PLA showed an obvious T_g at about
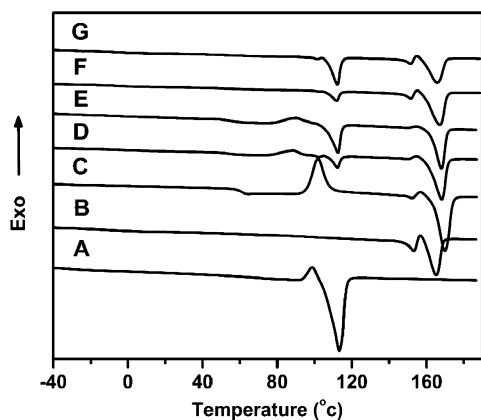

Figure 10. Second heating DSC thermograms for neat polymer and the ternary blends after cooling at 20 °C/min: (A) PBS; (B) PHBV; (C) PLA; (D) PLA/PHBV/PBS (60/30/10); (E) PLA/PHBV/PBS (60/10/30); (F) PHBV/PLA/PBS (60/30/10); (G) PHBV/PLA/PBS (60/10/30).

61.8 °C and a melting temperature of 169.8 °C. In addition, a broad exothermic peak corresponding to its cold crystallization was presented at 101.8 °C. Compared with the neat PLA, the cold crystallization temperature (T_{cc}) of PLA in the blends was found to shift toward a lower temperature region. These results indicate that the cold crystallization of PLA is promoted by the addition of PHBV and PBS, which is consistent with that of the DMA results. In general, cold crystallization took place at a temperature above the T_g of the blends at which the crystallizable polymer chains possessed enough segmental mobility to crystallize. The enhancement of cold crystallization of PLA by the addition of PHBV and PBS can be attributed to the following reason. First, as discussed in previous results, PHBV and PBS show limited miscibility with PLA. The amorphous phases of PHBV and PBS could activate the chain mobility of PLA. If there is sufficient chain mobility locally activated, the cold crystallization will be improved due to the easily dynamic chain alignment. Second, the surface of the PHBV and PBS domains might also act as a nucleating center and thereby enhance the crystallization of the PLA in the blends.[12,44,51] Recently, Yazawa et al. thoroughly studied the nucleation enhancement effect in the PLA/PCL blend, which was a system with some limited compatibility.[52] The author pointed out that the phase interface seems to play a pivotal role in the nucleation enhancement effect in the blends. They suggested that the aggregated PCL domains could facilitate a local and deep depression of T_g at the interface, thereby, resulting in nucleation at the interface of the domains. In polymer blends, the influence of the interface between the phase-separated domains on the crystallization should be considered seriously.[53,54] The chain of the polymer segments near the interface will be different from that of the segment in bulk at two aspects due to the presence of the interface in multiphase systems. First, an enrichment of chain ends, the shorter chains of the components and small third-molecule at the vicinity of the interface will improve the chain mobility of the polymer segments near the interface. Second, an enhancement of orientational ordering of polymeric coils may occur near the interface in the blends. Several researches had found that the enhanced segmental mobility near the free surface might result in an enhanced local ordering of the near-surface chain.[53,55,56] Such localized alignment could act as a precursor to crystallization. In poly(dimethylsiloxane) composites, Dollase and his co-workers suggested that regions of non-random chain conformations on intermediate length scales near the interface may play an important role in the early stages of crystallization, even if the orientational ordering of these regions does not match that of the lowest energy crystalline phase.[53] These regions may offer a different pathway for crystallization by allowing the system to bypass kinetic barriers that delay crystallization. In a semicrystalline polymer such as poly(ethylene terephthalate) (PET), an enhanced mobility at the surface in tandem with localized alignment was found to lead to a lower cold crystallization temperature and increased kinetics at the free surface.[57,58] These results had important implications for our understanding of the behavior of polymer systems near interfaces. Similar to the PLA/PCL blend, PLA/PHBV/PBS ternary blend is also a system with some degree of compatibility. Therefore, it is reasonable to speculate that the presence of PHBV and PBS phase could play a role of nucleation for PLA. No obvious change can be observed for the melting behavior of PBS in the blends compared to that of neat PBS. As for the melting behavior of PHBV and PLA, since the

3098

dx.doi.org/10.1021/am3004522 | ACS Appl. Mater. Interfaces 2012, 4, 3091–3101

fusion peaks of PHBV and PLA are located almost at the same temperature, it is difficult for the fusion peaks of the blends to be distinguished into each component peak. The bimodal melting peaks could be observed for the neat polymer and blends, which may result from melt-recrystallization mechanism. During the slow DSC scans, the less perfect crystals got enough time to melt and reorganized into crystals with higher structure perfection and remelt at higher temperature.

It is well-known that crystallization behavior of PLA is important both for end-use and for manufacturing of PLA, since in amorphous form, the range of application of PLA is severely limited by its low glass transition temperature, and the slow crystallization rate will limit the processabilty of PLA. To clarify the influence of PHBV and PBS on the crystallization behavior of PLA from melting state, the samples were also cooled from the crystal free melt at a cooling rate of 2 °C/min by DSC, and the cooling traces are shown in Figure 11. When
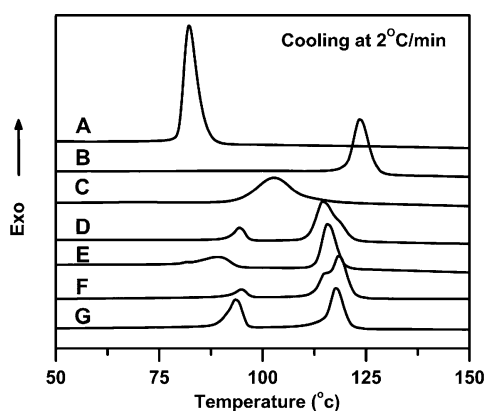

Figure 11. Cooling DSC thermograms at cooling rate 2 °C/min for neat polymer and the blends after melted at 190 °C for 3 min: (A) PBS; (B) PHBV; (C) PLA; (D) PLA/PHBV/PBS (60/30/10); (E) PLA/PHBV/PBS (60/10/30); (F) PHBV/PLA/PBS (60/30/10); (G) PHBV/PLA/PBS (60/10/30).

the cooling rate was 2 °C/min, an obvious exothermic peak due to the crystallization of PLA was observed at about 98 °C for neat PLA. Regarding the ternary blends with only 10% PHBV or 10% PLA, we could not strictly distinguish each component peak for PHBV and PLA because the exothermic peaks due to crystallization of PLA and PHBV overlapped. However, we can clearly analyze the crystallization behavior of PLA in the blends PLA/PHBV/PBS 60/30/10 and PHBV/PLA/PBS 60/30/10. As shown in Figure 11, the DSC cooling scan of the blends revealed all the three exothermic peaks corresponding to the crystallization of the component polymers. Compared with neat PLA, the T_c of PLA in the blends shifted to a higher temperature region indicating that the crystallization of PLA was promoted in the blends. Here the enhancement of crystallization of PLA in the blends may be attributed to the same reason as that of PBS.

3.7. Wide-Angle X-ray Diffraction and Crystal Structures of the Blends. The crystal structures of the three neat polymers and the ternary blends were characterized by X-ray diffraction. Considering that the processing methods used to fabricate the final products of polymers such as injection molding are in nonisothermal history, the crystal structure of the blends formed from melt state under the nonisothermal conditions were investigated. Figure 12 shows the wide-angle X-ray diffraction (WAXD) patterns of melt-crystallized samples
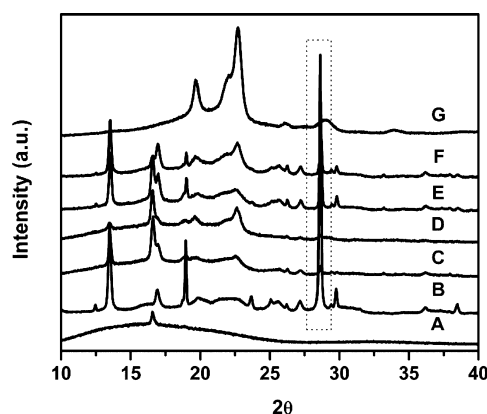

Figure 12. Typical wide-angle X-ray diffraction (WAXD) patterns of the neat polymers and blends: (A) PLA; (B) PHBV; (C) PLA/PHBV/PBS (60/30/10); (D) PLA/PHBV/PBS (60/10/30); (E) PHBV/PLA/PBS (60/30/10); (F) PHBV/PLA/PBS (60/10/30); (G) PBS.

at the cooling rate of 20 °C/min. Only one weak diffraction peak at around 16.5° is observed for neat PLA indicating the poor crystal formed under the nonisothermal history. Neat PHBV presents two strong diffraction peaks at around 12.9 and 16.3° corresponding to the (020) and (110) planes of the orthorhombic unit cell.[49,50] The very strong diffraction peak marked by dotted line rectangular box here was attributed the crystal of inorganic filler consisting in the PHBV material. PBS shows three strong diffraction peaks located at 2θ values of 19.6, 21.9, and 22.7°, which can be assigned to the (020), (010), and (110) planes of its monoclinic unit cell, respectively.[59] For the ternary blends, all the diffraction peaks of each component were clearly seen at the same positions. The absence of peaks shifts suggests that the PLA, PHBV, and PBS crystallized separately in the blends. However, the intensity of the diffraction peaks of the components varied with the composition of the components in the blends. Compared with that of neat PLA, strong diffraction peaks with higher intensity were clearly observed at 16.5° because of the diffractions from (200)/(100) planes. This indicates that the crystallization of PLA was enhanced in the blend, which is consistent with DSC results.

3.7. Heat Deflection Temperature. The HDT represents the upper working temperature limit of a plastic and is defined as the temperature at which a material will deflect 0.25 mm under the load of 0.455 MPa.[60] Table 3 reveals the HDT data of PLA, PHBV, and the ternary blends obtained under a load of 0.455 MPa. The pure PHBV and PLA have the HDT of 115 and 55.2 °C, respectively, which is reasonable as explained by Kawamoto et al. that the HDT of an amorphous polymer is around its glass transition temperature and that of a highly crystalline polymer is at the vicinity of its melting point.[61] In

Table 3. Heat Deflection Temperature (HDT) of Neat Polymer and the Blends

sample (wt/wt/wt)	T (°C)
neat PLA	55.2 ± 0.2
neat PHBV	115 ± 0.5
PLA/PHBV/PBS(60/30/10)	58.9 ± 0.3
PLA/PHBV/PBS (60/10/30)	58.4 ± 0.1
PHBV/PLA/PBS (60/30/10)	72.2 ± 0.1
PHBV/PLA/PBS(60/10/30)	87.5 ± 0.3

the present study, for the blends with PLA as matrix, there was a limited improvement in HDT from 55 to 58 °C by incorporation of PHBV and PBS. It seems that the HDT of PLA governs the overall thermal resistance of the ternary blends with PLA as matrix. The limited temperature increase here may be due to the increase in crystallization ability of PLA in the blends. When the content of PHBV increased, the HDT increased to a higher temperature.

3.8. Melt Flow Index (MFI). The melt flow index measurement was an important method to characterize the processing properties of polymer melt. The results of the MFI measurements are represented in Table 4. The MFR of PLA

Table 4. Melt Flow Index (MFI) of Neat Polymer and the Blends

sample (wt/wt/wt)	MFI (190 °C) g/10 min
neat PLA	32 ± 1.3
neat PHBV	13.9 ± 2.0
neat PBS	30.1 ± 1.5
PLA/PHBV/PBS(60/30/10)	34.5 ± 2.5
PLA/PHBV/PBS (60/10/30)	35.1 ± 3.2
PHBV/PLA/PBS (60/30/10)	28.5 ± 2.1
PHBV/PLA/PBS(60/10/30)	29.1 ± 1.3

and PBS show similar value above 30 g/10 min, whereas high viscosity is observed for PHBV with a value at 13.9 g/10 min. For the blends with PLA as matrix, only a slightly increase of MFI are observed which may be due to the decrease in the polymer molecular weight and thermal properties during mixing at the high process temperature. However, MFI of the blends with PHBV as matrix increased sharply compared to neat PHBV, two times higher value are achieved. The MFI results indicate that the blends show more excellent flow behavior compared to neat polymer, which are beneficial for the filler or fiber-reinforced composites uses.

4. CONCLUSION

We first reported a novel fully biodegradable PLA/PHBV/PBS ternary blend with the aim of obtaining high performance materials. The ternary blends exhibited unique synergistic mechanical properties which are not seen in either of the homopolymers or their binary blends. Mechanical analysis revealed that dispersions of PHBV and PBS minor phases improve remarkably the flexibility and impact strength with reducing the elastic modulus of the PLA matrix slightly. More interestingly, a good balance of stiffness and toughness was attained for PHBV/PLA/PBS ternary blends with PHBV as matrix. The failure mode changed from brittle fracture of the neat PLA to ductile fracture of the blends as demonstrated by the SEM micrographs of impact-fracture surface. DMA results indicated that PHBV and PLA are partially miscible system, whereas both of them showed limited compatibility with PBS. Enhancement in crystallization of PLA and PBS was achieved by incorporating PHBV phases, whereas the crystallization of PHBV in the blends was suppressed by PBS and PLA. Phase-separated minor phase morphology was observed from SEM results for all the blends' composition except PHBV/PLA/PBS 60/30/10 blend, which formed a typical mixture of core–shell morphology. The thermal resistance of PLA was improved by the addition of PHBV and PBS. The blends with PHBV as matrix showed more good thermal resistance than that of PLA matrix blends. Based on the mechanical and HDT results, the

PHBV/PLA/PBS 60/30/10 blend shows the optimum performance with excellent balanced stiffness-toughness and thermal resistance.

AUTHOR INFORMATION

Corresponding Author

*Tel.: +1 519 824 4120, ×56664. Fax: +1 519 763 8933. E-mail: mohanty@uoguelph.ca (A.K.M.); mmisra@uoguelph.ca (M.M.).

Notes

The authors declare no competing financial interest.

REFERENCES

(1) Yu, L.; Dean, K.; Li, L. *Prog. Polym. Sci.* **2006**, *36*, 576−602.
(2) Chen, G. Q.; Patel, M. K. *Chem. Rev.* **2012**, DOI: 10.1021/cr200162d.
(3) Mohanty, A. K.; Misra, M.; Drzal, L. T. *J. Polym. Environ.* **2002**, *10*, 19−26.
(4) Williams, C. K.; Hillmyer, M. A. *Polym. Rev.* **2008**, *48*, 1−10.
(5) Kijchavengkul, T.; Auras, R. *Polym. Int.* **2008**, *57*, 793−804.
(6) Rajeev, M.; Vineet, K.; Haripada, B.; Upadhyay, S. N. *J. Macromol. Sci, Part C: Polym. Rev.* **2005**, *45*, 325−349.
(7) Lim, L. T.; Auras, R.; Rubino, M. *Prog. Polym. Sci.* **2008**, *33*, 820−852.
(8) Kelly, S. A.; Kathleen, M. S.; Hillmyer, M. A. *Polym. Rev.* **2008**, *48*, 85−108.
(9) Liu, H.; Zhang, J. *J. Polym. Sci., Part B: Polym. Phys.* **2011**, *49*, 1051−1083.
(10) Bhardwaj, R.; Mohanty, A. K. *Biomacromolecules* **2007**, *8*, 2476−2484.
(11) Lin, Y.; Zhang, K. Y.; Dong, Z. M.; Dong, L. S.; Li, Y. S. *Macromolecules* **2007**, *40*, 6257−6267.
(12) Zhang, K.; Ran, X.; Wang, X.; Han, C.; Han, L.; Wen, X.; Zhuang, Y.; Dong, L. *Polym. Eng. Sci.* **2011**, *51*, 2370−2380.
(13) Shibata, M.; Inoue, Y.; Miyoshi, M. *Polymer* **2006**, *47*, 3557−3564.
(14) Lenz, R. W.; Marchessault, R. H. *Biomacromolecules* **2005**, *6*, 1−8.
(15) Doi, Y.; Segawa, A.; Nakamura, S.; Kunioka, M. Production of biodegradable copolyesters by Alcaligenes eutrophus. In *Novel Biodegradable Microbial Polymers*; Dawes, E. A., Ed.; Kluwer Academic: Dordrecht, The Netherlands, 1990; pp 37−48.
(16) Braunegg, G.; Lefebvre, G.; Genser, K. F. *J. Biotechnol.* **1998**, *65*, 127−161.
(17) Kunioka, M.; Tamaki, A.; Doi, Y. *Macromolecules* **1989**, *22*, 694−697.
(18) Ha, C. S.; Cho, W. J. *Prog. Polym. Sci.* **2002**, *27*, 759−809.
(19) Ichikawa, Y.; Mizukoshi, T. *Adv. Polym. Sci.* **2012**, *245*, 285−313.
(20) Xu, J.; Guo, B. H. *Biotechnol. J.* **2010**, *5*, 1149−1163.
(21) Myriant Technologies websites. Available at: http://www.myriant.com/succinicpage.htm
(22) Harada, M.; Ohya, T.; Iida, K.; Hayashi, H.; Hirano, K.; Fukuda, H. *J. Appl. Polym. Sci.* **2007**, *106*, 1813−1820.
(23) Park, J. W.; Im, S. S. *J. Appl. Polym. Sci.* **2002**, *86*, 647−655.
(24) Yokohara, T.; Yamaguchi, M. *Eur. Polym. J.* **2008**, *44*, 677−685.
(25) Yokohara, T.; Okamoto, K.; Yamaguchi, M. *J. Appl. Polym. Sci.* **2010**, *117*, 2226−2232.

3100

dx.doi.org/10.1021/am3004522 | *ACS Appl. Mater. Interfaces* 2012, 4, 3091−3101

(26) Wang, R.; Wang, S.; Zhang, Y.; Wan, C.; Ma, P. *Polym. Eng. Sci.* **2009**, *49*, 26−33.

(27) Park, E. S.; Kim, H. K.; Shim, J. H.; Kim, H. S.; Jang, L. W.; Yoon, J. S. *J. Appl. Polym. Sci.* **2004**, *92*, 3508−3513.

(28) Ferreira, B. M. P.; Zavaglia, C. A. C.; Duek, E. A. R. *J. Appl. Polym. Sci.* **2002**, *86*, 2898−2906.

(29) Nanda, M. R.; Misra, M.; Mohanty, A. K. *Macromol. Mater. Eng.* **2011**, *296*, 719−728.

(30) Wang, S.; Ma, P.; Wang, R.; Wang, S.; Zhang, Y.; Zhang, Y. *Polym. Degrad. Stab.* **2008**, *93*, 1364−1369.

(31) Iannace, S.; Ambrosio, L.; Huang, S. J.; Nicolais, L. *J. Appl. Polym. Sci.* **1994**, *54*, 1525−1536.

(32) Luzinov, I.; Pagnoulle, C.; Jerome, R. *Polymer* **2000**, *41*, 7099−7109.

(33) Shokoohi, S.; Arefazar, A. *Polym. Adv. Technol.* **2009**, *20*, 433−447.

(34) Ticiane, S. V.; Augusto, T. M.; Nicole, R. D. *Macromolecules* **2006**, *39*, 2663−2675.

(35) Joe, R.; Basil, D. F. *Macromolecules* **2000**, *33*, 6998−7008.

(36) Guo, H. F.; Packirisamy, S.; Gvozdic, N. V.; Meier, D. J. *Polymer* **1997**, *38*, 785−794.

(37) Hobbs, S. Y.; Dekkers, M. E. J.; Watkins, V. H. *Polymer* **1988**, *29*, 1598−1602.

(38) Nemirovski, N.; Siegmann, A.; Narkis, M. *J. Macromol. Sci., Phys.* **1995**, *B34*, 459−475.

(39) Luzinov, I.; Xi, K.; Pagnoulle, C.; Huynh-Ba, G.; Jerome, R. *Polymer* **1999**, *40*, 2511−2520.

(40) Wu, S. *J. Polym. Sci., Part C: Polym. Symp.* **1971**, *34*, 19−30.

(41) Abolhasani, M. M.; Arefazar, A.; Mozdianfard, M. *J. Polym. Sci., Part B: Polym. Phys.* **2010**, *48*, 251−259.

(42) Liu, H.; Song, W.; Chen, F.; Guo, L.; Zhang, J. *Macromolecules* **2011**, *44*, 1513−1522.

(43) Li Y., L.; Shimizu, H. *ACS Appl. Mater. Interfaces* **2009**, *1*, 1650−1655.

(44) Jiang, L.; Wolcott, M. P.; Zhang, J. *Biomacromolecules* **2006**, *7*, 199−207.

(45) Schwach, E.; Avérous, L. *Polym. Int.* **2004**, *53*, 2115−2124.

(46) Biresaw, G.; Carriere, C. J. *J. Polym. Sci., Part B: Polym. Phys.* **2001**, *39*, 920−930.

(47) Chun, Y. S.; Kim, W. N. *Polymer* **2000**, *41*, 2305−2308.

(48) Qiu, Z.; Ikehara, T.; Nishi, T. *Polymer* **2003**, *44*, 7519−7527.

(49) Miao, L.; Qiu, Z.; Yang, W.; Ikehara, T. *React. Funct. Polym.* **2008**, *68*, 446−457.

(50) Qiu, Z.; Yang, W.; Ikehara, T.; Nishi, T. *Polymer* **2005**, *46*, 11814−11819.

(51) Tsuji, H.; Sawada, M.; Bouapao, L. *ACS Appl. Mater. Interfaces* **2009**, *1*, 1719−1730.

(52) Sakai, F.; Nishikawa, K.; Inoue, Y.; Yazawa, K. *Macromolecules* **2009**, *42*, 8335−8342.

(53) Dollase, T.; Wilhelm, M.; Spiess, H. W.; Yagen, Y.; Yerushalmi-Rozen, R.; Gottlieb, M. *Interface Sci.* **2003**, *11*, 199−209.

(54) Mayes, A. M. *Macromolecules* **1994**, *27*, 3114−3115.

(55) Roth, C. B.; McNerny, K. L.; Jager, W. F.; Torkelson, J. M. *Macromolecules* **2007**, *40*, 2568−2574.

(56) Factor, B. J.; Russell, T. P.; Toney, M. F. *Phys. Rev. Lett.* **1991**, *66*, 1181−1184.

(57) Jukes, P. C.; Das, A.; Durell, M.; Trolley, D.; Higgins, A. M.; Geoghegan, M. J.; Macdonald, E.; Jones, R.; Brown, S.; Thompson, P. *Macromolecules* **2005**, *38*, 2315−2320.

(58) Lee, D. H.; Park, K. H.; Kim, Y. H.; Lee, H. S. *Macromolecules* **2007**, *40*, 6277−6282.

(59) Gan, Z. H.; Abe, H.; Kurokawa, H; Doi, Y. *Biomacromolecules* **2001**, *2*, 605−613.

(60) Turi, E. A. *Thermal Characterization of Polymeric Materials*, 2nd ed.; Academic Press: New York, 1997, p 793.

(61) Kawamoto, N.; Sakai, A.; Horikoshi, T.; Urushihara, T.; Tobita, E. *J. Appl. Polym. Sci.* **2007**, *103*, 244−250.